Appeared in Proc. of International Conference on Biometric Authentication (ICBA), LNCS vol. 3072, pp. 249-255, Hong Kong, July 2004.

Estimating Fingerprint Deformation

Arun Ross[1], Sarat C. Dass[2], Anil K. Jain[2]

[1] West Virginia University, Morgantown, WV 26506 USA
[2] Michigan State University, East Lansing, MI 48824 USA
ross@csee.wvu.edu, {sdass,jain}@msu.edu

Abstract. Fingerprint matching is affected by the nonlinear distortion introduced in fingerprint impressions during the image acquisition process. This nonlinear deformation causes fingerprint features such as minutiae points and ridge curves to be distorted in a complex manner. In this paper we develop an *average* deformation model for a fingerprint impression (baseline impression) by observing its relative distortion with respect to several other impressions of the same finger. The deformation is computed using a Thin Plate Spline (TPS) model that relies on ridge curve correspondences between image pairs. The estimated average deformation is used to distort the minutiae template of the baseline impression *prior* to matching. An index of deformation has been proposed to select the average deformation model with the least variability corresponding to a finger. Preliminary results indicate that the average deformation model can improve the matching performance of a fingerprint matcher.

1 Introduction

Automatic fingerprint matching involves determining the degree of similarity between two fingerprint impressions by comparing their ridge structure and/or the spatial distribution of the minutiae points. When direct-contact fingerprint sensors are used, the image acquisition process introduces non-linear distortions in the ridge structure due to the non-uniform finger pressure applied by the subject on the sensor and the elastic nature of the human skin. For reliable matching, these non-linear deformations must be accounted for prior to comparing two fingerprint images. Deformation models based on affine transformations invariably lead to unsatisfactory matching results since the distortions are basically elastic in nature. Thus, alternate techniques to handle such distortions have been suggested in the literature (see, for example, [1–6]). However, almost all techniques proposed thus far deal with the problem of non-linear distortion on a case by case basis, i.e., for *every* pair of fingerprint impressions (or for *every* fingerprint impression), a distortion removal technique is applied. No attempt has been made to develop a *finger-specific deformation model* that can be computed offline and then used during matching. The main advantage of an offline technique is that once a finger-specific model has been computed, recomputation of the model is not necessary during the matching stage. In this paper we describe an *average* deformation model for a fingerprint impression (baseline impression) by observing its relative distortion with respect to several other impressions of the same finger. The distortion is estimated using ridge curve correspondence between pairs of fingerprint impressions. The estimated average deformation is then used to distort the template minutiae set prior to matching it with that of a previously unseen query fingerprint. We also propose an index of deformation for ranking the average deformation models corresponding to every impression of a finger.

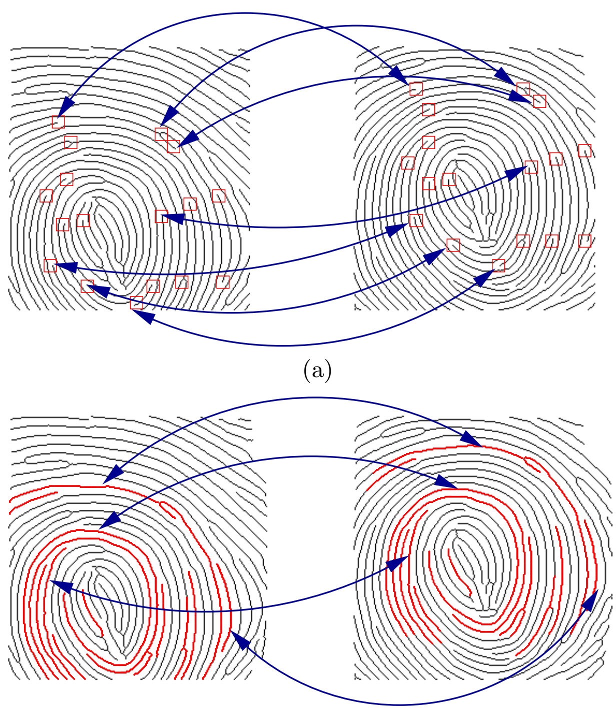

(a)

(b)

Fig. 1. (a) Minutiae point correspondences and (b) ridge curve correspondences between two impressions of a finger.

2 The Fingerprint Warping Model

Given a pair of grayscale fingerprint images, I_0 and I_1, we first obtain their thinned versions, R_0 and R_1. A thinned image is a binary image with grayscale values of 0 (indicating valleys) and 255 (indicating ridges). Each thinned image can be thought of as a collection of ridge curves. Minutiae points are then extracted from R_0 and R_1 resulting in two minutiae sets $M_0 = (m_{0,1}, m_{0,2}, \ldots, m_{0,k_0})$

and $M_1 = (m_{1,1}, m_{1,2}, \ldots, m_{1,k_1})$ of cardinalities k_0 and k_1, respectively. Here, each minutiae point $m_{i,j}$ is characterized by its location in the image, the orientation of the associated ridge, and the grayscale intensity of pixels in its vicinity. Minutiae correspondences between M_0 and M_1 are obtained using the elastic string matcher described in [7]. The output of this matcher is a similarity score in the range [0,1000] and a set of correspondences of the form $C = \{(m_{0,a_j}, m_{1,b_j}) : j = 1, 2, \ldots, k\}$ where $k \leq \min\{k_0, k_1\}$, and the a_js (b_js) are all distinct. Figure 1(a) shows an example of the minutiae point correspondences between two impressions of a finger. Once the correspondence between M_0 and M_1 has been established, the ridge curves associated with these minutiae points are extracted from R_0 and R_1 using a simple ridge tracing technique. A minutiae point that is a ridge ending has one ridge curve associated with it while a ridge bifurcation has three associated ridge curves (Figure 1(b)).[3]

Having determined the corresponding ridge curves, we next establish a correspondence between *points* on these curves by sampling every q-th point ($q = 20$) on each of the ridge curves. We denote this set of corresponding ridge points by $\mathcal{U} = (u_1^*, u_2^*, \ldots, u_N^*)^T$ and $\mathcal{V} = (v_1^*, v_2^*, \ldots, v_N^*)^T$. We use the thin plate spline (TPS) model to estimate the non-linear deformation F based on these points. TPS represents a natural parametric generalization from rigid to mild non-rigid deformations. The deformation model for TPS is given in terms of the warping function $F(u)$, with $F(u) = c + A \cdot u + W^T s(u)$, where $u \in R^2$, c is a 2×1 translation vector, A is a 2×2 affine matrix, W^T is a $N \times 2$ coefficient matrix, and $s(u) = [\sigma(u - u_1^*), \sigma(u - u_2^*), \ldots, \sigma(u - u_N^*)]^T$. Here, $\sigma(u) = ||u||^2 \log(||u||)$ if $||u|| > 0$ and $\sigma(u) = 0$, otherwise. There are 6 and $2N$ parameters corresponding to the affine[4] and non-linear parts of the deformation model, respectively, resulting in a total of $2N + 6$ parameters to be estimated. The restriction $F(u_j^*) = v_j^*$, $j = 1, 2, \ldots, N$ provides $2N$ constraints. For the parameters to be uniquely estimated, we further assume that W satisfies the two conditions (i) $1_N^T W = 0$ and (ii) $U_s^T W = 0$, where 1_N is the vector of ones of length N. Thus, the parameters of the TPS model can be obtained from the matrix equation

$$\begin{bmatrix} H & 1_N & \mathcal{U} \\ 1_N^T & 0 & 0 \\ \mathcal{U}^T & 0 & 0 \end{bmatrix} \begin{bmatrix} W \\ c^T \\ A^T \end{bmatrix} = \begin{bmatrix} \mathcal{V} \\ 0 \\ 0 \end{bmatrix}, \tag{1}$$

where H is the $N \times N$ matrix with entries $h_{ij} = \sigma(u_i^* - u_j^*)$. This gives rise to a TPS model that minimizes the bending energy subject to the perfect alignment constraint (i.e., $F(u_j^*) = v_j^*$). A more robust TPS model can be obtained by relaxing this constraint, and instead determining the function F which minimizes the expression

$$\sum_{j=1}^{N} (v_j^* - F(u_j^*))^T (v_j^* - F(u_j^*)) + \lambda J(F), \tag{2}$$

[3] Ridge endings and ridge bifurcations may be interchanged in the thinned image. We do account for such anomalies when determining ridge curve correspondences.

[4] The affine parameters are determined using minutiae point correspondences only and not the ridge point correspondences.

where $J(F) = \sum_{j=1}^{2} \int_{(x,y)} \left\{ \left(\frac{\partial^2 F_j(x,y)}{\partial x^2}\right)^2 + 2\left(\frac{\partial^2 F_j(x,y)}{\partial x \partial y}\right)^2 + \left(\frac{\partial^2 F_j(x,y)}{\partial y^2}\right)^2 \right\} dx\, dy$ represents the bending energy associated with $F = (F_1, F_2)^T$, F_j is the j^{th} component of F, and $\lambda > 0$. The case $\lambda = 0$ gives rise to the TPS model described by equation (1). For general $\lambda > 0$, the parameters of the resulting TPS model can be obtained using equation (1) with H replaced by $H + \lambda I_N$, where I_N is the $N \times N$ identity matrix.

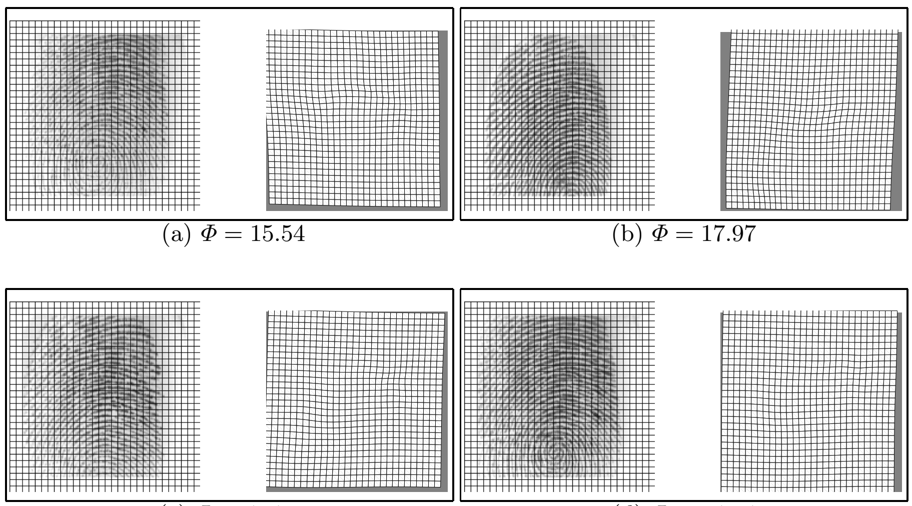

(a) $\Phi = 15.54$ (b) $\Phi = 17.97$

(c) $\Phi = 48.79$ (d) $\Phi = 94.34$

Fig. 2. The average deformation model (shown as deformations on a reference grid) corresponding to 4 templates of a finger sorted in increasing Φ-values. (a) is chosen to be the optimal template since it has the least Φ-value.

3 Average Deformation Model

Suppose we have L impressions of a finger, $T_1, T_2, \ldots, T_L$. Each impression, T_i, can be paired with the remaining impressions to create $L-1$ pairs of the form (T_i, T_j), $j \neq i$. For the pair (T_i, T_j), we obtain a non-linear transformation F_{ij} by employing the technique described in section 2. Note that F_{ij} transforms *every* pixel in the template fingerprint, T_i, to a new location. Thus, we can compute the *average* deformation of each pixel u in T_i as, $\bar{F}_i(u) = \frac{1}{L-1} \sum_{j \neq i} F_{ij}(u)$. There will be L average deformation models corresponding to the L impressions of the finger. The average deformation is the typical deformation that arises when we compare one fingerprint impression of a finger (the baseline impression) with other impressions of the same finger. Figure 2 shows that changing the baseline impression for the finger will result in a different average deformation model for that finger (the Φ values are discussed in section 3.1). Figure 3 shows the average deformation for 3 different fingers; it can be clearly seen that the average warping functions are different for the 3 fingers indicating that the fingerprint deformation is finger-specific.

3.1 The Φ Index of Deformation

We suggest a method to rank the average deformation models pertaining to multiple impressions of a finger. In order to do this, we first define the pixel-wise covariance matrix associated with the i-th average deformation, $\bar{F}_i$, as follows: $D_{\bar{F}_i}(u) = \frac{1}{L-1}\sum_{j\neq i}(F_{ij}(u) - \bar{F}_i(u)) \cdot (F_{ij}(u) - \bar{F}_i(u))^T$. Here, F_{ij} is the deformation function that warps T_i to T_j. The covariance matrix defined at each pixel u, is a measure of the variability associated with the estimated deformation functions. Two choices of pixel-wise measures of variability are given by (i) the determinant, $\phi(D_{\bar{F}_i}(u)) = |D_{\bar{F}_i}(u)|$, and (ii) the trace, $\phi(D_{\bar{F}_i}(u)) = \mathrm{tr}(D_{\bar{F}_i}(u))$. Pixels with large (small) values of ϕ indicate high (low) variability in the deformations F_{ij}. We propose to use the values of ϕ to determine the optimal model for a given finger. We define the i^{th} index of deformation, Φ_i, as $\Phi_i = \frac{1}{|S|}\sum_{u=1}^{|S|} \phi(D_{\bar{F}_{i(u)}})$, where, $\phi(D) = tr(D)$, and $|S|$ is the number of pixels in the image. Subsequently, we choose T_{i^*} as the template with the smallest variability in deformation if $i^* = \arg\min_i \Phi_i$. In effect, we choose that template T_i that minimizes the average variation across pixels measured in terms of Φ_i. Low (high) values of the index of deformation indicate that the warping functions are similar (dissimilar) to each other.

4 Experimental Results

In order to reliably estimate fingerprint deformation, we need several impressions of the same finger (~ 16). Large number of impressions per finger are not available in standard fingerprint databases (e.g., FVC 2002 and NIST). Therefore, fingerprint images of 50 fingers were acquired using the Identix sensor (256×255, 380 dpi) over a period of two weeks in our lab. There were 32 impressions corresponding to every finger, resulting in a total of $1,600$ impressions. One half of the impressions ($L = 16$ for each finger, resulting in 800 impressions) were used as templates to compute the average deformation model for each finger, while the remaining 800 impressions were used as query images for testing. For each template image, T, the minutiae set, M_T, and the thinned image, R_T, were extracted. The average deformation model of T, $\bar{F}_T$, was obtained based on pairings with the remaining 15 impressions of the same finger (equation (2) with $\lambda = 0.1$). The minutiae set M_T was transformed to the deformed set, $MD_T \equiv \bar{F}_T(M_T)$ using $\bar{F}_T$. A total of 800 sets (50×16) of deformed minutiae points were thus obtained. In order to test the matching performance of the deformed minutiae sets, and the utility of the index of deformation, Φ, the following two experiments were conducted.

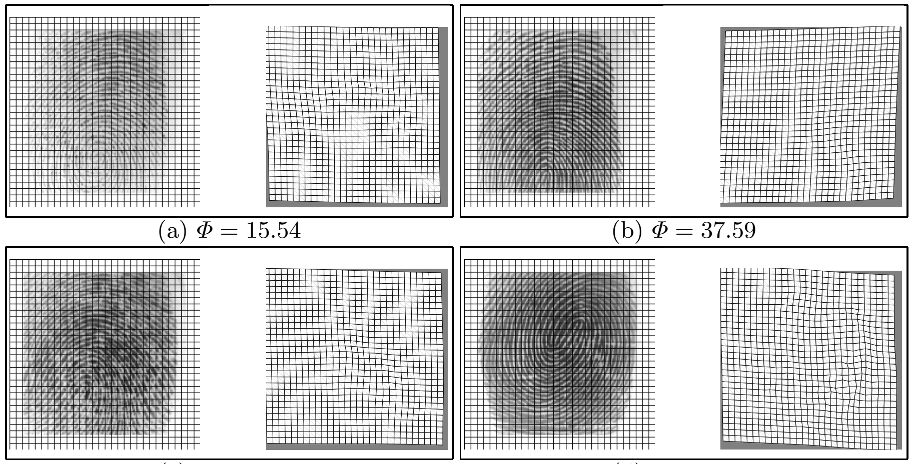

(a) $\Phi = 15.54$ (b) $\Phi = 37.59$

(c) $\Phi = 85.18$ (d) $\Phi = 35.30$

Fig. 3. The average deformation model (shown as deformations on a reference grid) of 4 different fingers.

In the first experiment, the matching performance using the average deformation model was evaluated. Every template image, T, was compared with every query image, Q, and two types of matching scores [7] were generated for each comparison: the matching score obtained by matching (i) M_T with M_Q, and (ii) MD_T with M_Q. The Receiver Operating Characteristic (ROC) curve plotting the genuine accept rate (GAR) against the false accept rate (FAR) at various matching thresholds is presented in Figure 4(a). An overall improvement of 2% is observed when the average deformation model is used to distort M_T prior to matching. In the second experiment, the advantage of using the index of deformation is demonstrated. The Φ-index of deformation (with $\phi(D) = \text{tr}(D)$) is used to rank the templates according to variability in the distortion. The template images can now be split into two sets: (i) impressions with the least Φ values for every finger (the Φ-optimal templates) and (ii) the remaining impressions for every finger (the Φ-suboptimal templates). We repeated the matching procedure outlined above using these two template sets. The resulting ROC curve is shown in Figure 4(b). From the figure, it is clear that using Φ-optimal templates results in better performance compared to using Φ-suboptimal templates. Further, the Φ-suboptimal templates still yield better performance compared to the non-distorted templates thus demonstrating the importance of the average deformable model.

5 Summary and Future Work

In this paper, an average deformation model for fingerprint impressions has been proposed. The proposed technique has been shown to improve the performance

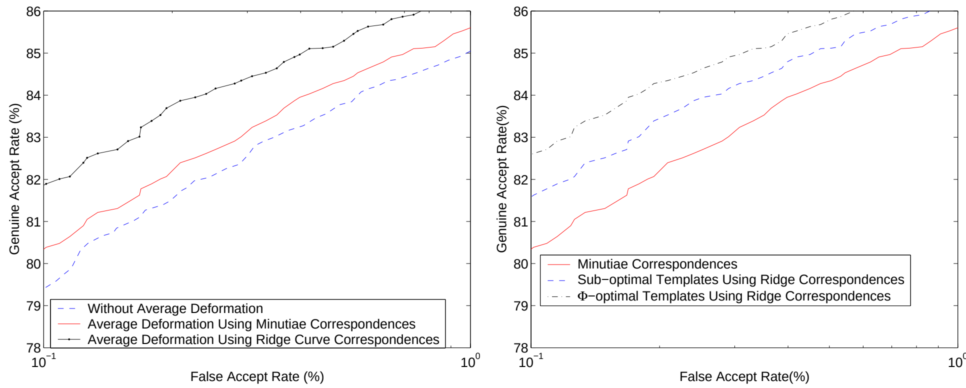

(a) (b)

Fig. 4. (a) Improvement in matching performance when ridge curve correspondences is used to develop the average deformation model. (b) Matching performance when the Φ index of deformation is used to select optimal templates.

of a fingerprint matching system. An index of deformation has been suggested to select the "optimal" average deformation model corresponding to multiple impressions of a finger. Future work includes adopting an incremental approach to updating the average deformation model, determining a more robust measure (than simple pixel-wise averaging) to compute the average deformation model, and employing curve matching techniques to establish ridge curve correspondences between image pairs.

References

1. Ratha, N.K., Bolle, R.M.: Effect of controlled acquisition on fingerprint matching. In: Proceedings of the International Conference on Pattern Recognition. Volume 2., Brisbane, Australia (1998) 1659–1661
2. Dorai, C., Ratha, N., Bolle, R.: Detecting dynamic behavior in compressed fingerprint videos: Distortion. In: Proceedings of Computer Vision and Pattern Recognition. (2000) 320–326
3. Kovács-Vajna, Z.M.: A fingerprint verification system based on triangular matching and dynamic time warping. IEEE Transactions on PAMI **22** (2000) 1266–1276
4. Bazen, A.M., Gerez, S.: Fingerprint matching by thin-plate spline modelling of elastic deformations. Pattern Recognition **36** (2003)
5. Senior, A., Bolle, R.: Improved fingerprint matching by distortion removal. IEICE Transactions on Information and Systems **E84-D** (2001) 825–831
6. Watson, C., Grother, P., Cassasent, D.: Distortion-tolerant filter for elastic-distorted fingerprint matching. In: Proceedings of SPIE Optical Pattern Recognition. (2000) 166–174
7. Jain, A.K., Hong, L., Bolle, R.: On-line fingerprint verification. IEEE Transactions on PAMI **19** (1997) 302–314